

Phase diagram of a cold polarized Fermi gas

D. T. Son¹ and M. A. Stephanov²

¹*Institute for Nuclear Theory, University of Washington, Seattle, Washington 98195-1550, USA*

²*Department of Physics, University of Illinois, Chicago, Illinois 60607-7059, USA*

(Dated: July 2005)

We propose a phase diagram for a cold polarized atomic Fermi gas with zero-range interaction. We identify four main phases in the plane of density and polarization: the superfluid phase, the normal phase, the gapless superfluid phase, and the modulated phase. We argue that there exists a Lifshitz point at the junction of the normal, the gapless superfluid, and the modulated phases, and a splitting point where the superfluid, the gapless superfluid, and the modulated phases meet. We show that the physics near the splitting point is universal and derive an effective field theory describing it. We also show that subregions with one and two Fermi surfaces exist within the normal and the gapless superfluid phases.

PACS numbers: 03.75.Ss

I. INTRODUCTION

The Fermi gas in the regime of large scattering length a [1–3] has attracted much interest due to its universal behavior. The regime can be achieved in atom traps by using the technique of Feshbach resonance [4–8]. Most attention is focused on systems consisting of two components of fermions (e.g., two spin components of a spin- $\frac{1}{2}$ fermion) with equal number density. When the effective range r_0 is small compared to the interparticle distance $n^{-1/3}$, where n is the total number density, many properties of the system depend on n and a only through the dimensionless diluteness parameter

$$\kappa = -\frac{1}{na^3}. \quad (1)$$

When one varies κ the system interpolates between the Bose-Einstein condensation (BEC) regime and the Bardeen-Cooper-Schrieffer (BCS) regime. For all values of κ the ground state is believed to be a superfluid.

In contrast, the case of unequal number density (or unequal chemical potentials) of the two components is much less understood [9–11]. In the case of spin- $\frac{1}{2}$ fermions one refers to a polarized gas. We follow this terminology, understanding “polarized” in the sense of asymmetry between the two components.

In this paper we propose a phase diagram for a polarized Fermi gas in the whole range from the BEC to the BCS regime. Our proposal is summarized in Fig. 1. There are two special points on the phase diagram. Point S (the splitting point) is a point where phases I, III and IV meet. Point L is a Lifshitz point where II, III and IV meet. The focus of this paper is on the point S . The physics in the vicinity of this point is of a long-distance, i.e., universal, nature and can be reliably studied within an effective field theory.

Our proposal for the global structure of the phase diagram is an educated guess anchored on the following reliable facts: the known phase structure in the BEC and BCS limits; the existence of the point S , which is at least a local minimum of the free energy; and the struc-

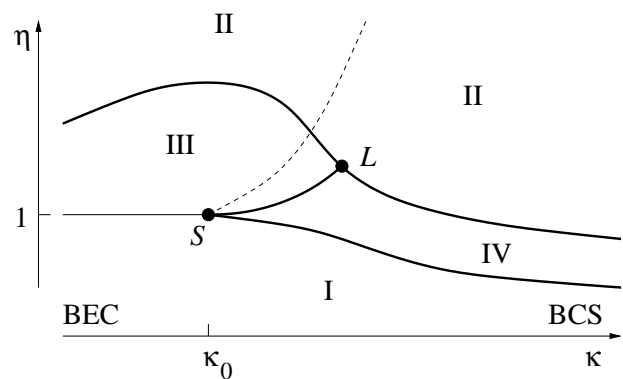


FIG. 1: The proposed phase diagram in the plane of the diluteness parameter $\kappa = -1/(na^3)$ and the (scaled) polarization chemical potential $\eta = H/\Delta_{H=0}$. I is the unpolarized BEC/BCS phase, II is the normal phase, III is the gapless superfluid phase, and IV is a region of Fulde-Ferrell-Larkin-Ovchinnikov phases. The dashed line divides phases II and III into regions with one (on the left) and two (on the right) Fermi surfaces. Region IV must be divided into phases with different patterns of breaking of the rotational symmetry (not shown).

ture of the phase diagram around S , studied in detail in this paper.

We devote the Appendix to the question of the global stability of the splitting point. We show that quantum Monte Carlo simulations [11] indicate that the superfluid state at point S is globally stable. We also argue that mean-field calculations of the phase diagram will likely miss the point S by significantly overestimating the size of the region occupied by phase II.

II. QUALITATIVE DESCRIPTION OF THE PHASE DIAGRAM

A. Axes of the phase diagram

A particular system is characterized by three parameters: the scattering length a and the chemical potentials

of the two components μ_\uparrow and μ_\downarrow . Because of universality (corresponding to rescaling invariance $a \rightarrow e^{-s}a$, $\mu_i \rightarrow e^{2s}\mu_i$) the whole phase diagram can be captured in a two-dimensional plot. We introduce the notation

$$\mu = \frac{1}{2}(\mu_\uparrow + \mu_\downarrow), \quad H = \frac{1}{2}(\mu_\uparrow - \mu_\downarrow). \quad (2)$$

Then the parameter κ on the horizontal axis is defined by Eq. (1) where $n = n(\mu, a)$ is the density of an unpolarized gas at chemical potential μ and scattering length a . Thus κ is the inverse diluteness parameter of an unpolarized system with chemical potential equal to the average of μ_\uparrow and μ_\downarrow and with the same scattering length a .

The parameter η on the vertical axis is defined as

$$\eta = \frac{H}{\Delta(\mu, a)}. \quad (3)$$

Here $\Delta(\mu, a)$ is the gap in the fermion excitation spectrum of the unpolarized gas. We divide H by Δ so that η is dimensionless. This is also convenient because $\eta = 1$ is the line dividing phases I and III, as explained below.

B. Qualitative understanding of the phase diagram

The general structure of the phase diagram can be guessed by studying the BEC and BCS limits first. In the BEC limit $\kappa \rightarrow -\infty$, the gap in the fermionic excitation spectrum is close to the two-body binding energy. The excitations are fermionic quasiparticles carrying charge $+1$ and -1 with respect to the chemical potential H . When $H < \Delta$ or $\eta < 1$, the ground state is the same as for $\eta = 0$ since it is energetically unfavorable to create an unbound fermion on top of the BEC ground state (phase I). However, if $\eta > 1$, extra fermions will be created, and the system, for a range of η , is a homogeneous mixture of bosonic bound states and fermions carrying one sign of spin (phase III). Finally, for sufficiently large η all bosonic bound states disappear and the system is a completely polarized Fermi gas (phase II).

The ground state in the BCS limit $\kappa \rightarrow +\infty$ is also known. For $\eta < \eta_1 \approx 1/\sqrt{2}$, the ground state remains the BCS state with zero polarization (I). For $\eta_1 < \eta < 0.754$, the ground state is in one of the Fulde-Ferrell-Larkin-Ovchinnikov (FFLO) states [12, 13] where Cooper pairs form with nonzero momentum and the superfluid order parameter varies in space (IV). The precise spatial structure of the ground state is difficult to determine, but it is presumably crystalline. Finally for $\eta > 0.754$ the system goes to the Fermi liquid phase II.

At small η , the unpolarized BEC phase can continue analytically into the unpolarized BCS phase. Indeed, in both regimes the U(1) symmetry associated with the conservation of the total number of atoms is spontaneously broken. At large η , the normal phase on the BEC side and that on the BCS side are essentially the same phase of a polarized Fermi gas. On both sides the U(1) symmetry is restored. However, at intermediate η the phases

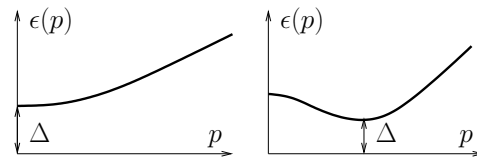


FIG. 2: Spectrum of fermionic quasiparticles at $\eta = 0$ for $\kappa < \kappa_0$ (left) and for $\kappa > \kappa_0$ (right). The minimum is located at $p = 0$ for $\kappa < \kappa_0$ and $p \neq 0$ for $\kappa > \kappa_0$.

in the two limits are qualitatively different: on the BCS side the translational invariance is spontaneously broken, while on the BEC side it is not, as already observed in Ref. [10].

Under the assumption that the phase diagram contains four phases which enter the region of intermediate κ and η —I from below, II from above, III from the left and IV from the right—there are two possibilities. The first is that there is a phase transition (coexistence) line separating the boson-fermion mixture phase III and the FFLO phase IV. The second is that III and IV do not coexist, but instead I and II do, which is what is found in mean-field theory. In the Appendix we argue that this is a likely artifact of the mean-field approximation.

Within the first possibility, the minimal phase diagram therefore should look like Fig. 1. The line which separates the mixture phase III from the FFLO phase IV should start at a point S located on the boundary of the unpolarized BEC/BCS phase I, and end at a point L on the boundary of the normal phase II. The point S will be called the splitting point, since, as we will show below, it is the point where the onset transition (from the unpolarized phase I to the mixture phase III) splits into two first-order phase transitions. The point L , by the nature of the phases surrounding it, is a Lifshitz point [14].

In the next section we shall identify the splitting point S and study the phases surrounding it. We shall see that the physics around S matches very well with the global picture presented above.

III. THE SPLITTING POINT

A. Location of the splitting point

Begin by considering the unpolarized gas, i.e., $\eta = 0$. The dispersion relation of a fermionic quasiparticle $\epsilon(\mathbf{p})$ has a finite gap Δ in the whole range of κ , from BEC to BCS. There is, however, a qualitative change in the location of the minimum of the dispersion curve as illustrated in Fig. 2. In the BEC limit the dispersion curve is $\epsilon(\mathbf{p}) = p^2/(2m) + \Delta$ and achieves its minimum at $p = 0$. On the other hand, in the BCS limit the dispersion curve has a minimum at $p \neq 0$ (near the Fermi momentum).

One concludes that, as the system crosses over from the BEC to the BCS regime, at a certain point $\kappa = \kappa_0$ the minimum of the dispersion curve shifts from $p = 0$

to $p \neq 0$. In the mean-field theory this occurs when the chemical potential vanishes [2]; we shall only assume that this transition occurs smoothly. Around this κ the dispersion curve has the following behavior near $p = 0$:

$$\epsilon(\mathbf{p}) = \epsilon_0 - \alpha p^2 + \beta p^4, \quad (4)$$

where α changes sign at $\kappa = \kappa_0$: $\alpha = \alpha_0(\kappa - \kappa_0)$, $\alpha_0 > 0$. Note that $\Delta = \epsilon_0 - \theta(\alpha)\alpha^2/(4\beta)$.

At $\eta = 0$, the change in the location of the minimum of the dispersion curve by itself does not signal any phase transition. However, as we shall see shortly, the splitting point S is located at $\kappa = \kappa_0$ and $\eta = 1$.

The value of κ_0 cannot be found from effective theory. One can determine the sign of κ from the shape of the dispersion curve at infinite scattering length ($\kappa = 0$). According to a recent quantum Monte-Carlo calculation [11], at $\kappa = 0$ the dispersion is BCS-like, i.e., has a minimum at a nonzero value of p . From this information we conclude that $\kappa_0 < 0$, i.e., on the left (BEC) side of the phase diagram in Fig. 1.

B. Effective field theory near the splitting point

Let us take the system at some κ close to κ_0 and increase η . When η is close to 1, there are fermion quasiparticles whose energy $\epsilon = \epsilon(\mathbf{p}) - H$ is small. The momenta of these quasiparticles are also small, around the minimum of the dispersion curves. At small number density, these quasiparticles are weakly interacting. The whole problem is therefore treatable by using a low-energy effective field theory of quasiparticles (superfluid phonons and the extra fermions) despite the fact that the original (undressed) particles are strongly coupled.

The effective Lagrangian is constrained by two U(1) symmetries. One of them corresponds to the conservation of the total number of atoms. The superfluid mode φ , which we normalize to be half of the phase of the Cooper pair, transforms under this symmetry as $\varphi \rightarrow \varphi + \alpha$. The fermion field ψ can always be chosen to be neutral under this symmetry by multiplying it by an appropriate power of $e^{i\varphi}$. Another U(1) symmetry corresponds to the conservation of the difference of the numbers of the two components, or polarization. Under this symmetry $\psi \rightarrow \psi e^{i\beta}$, while φ is invariant. To lowest nontrivial order in φ and ψ and derivatives the Lagrangian obeying these symmetries is given by

$$\mathcal{L} = \frac{f_t^2}{2}\dot{\varphi}^2 - \frac{f^2}{2}(\partial\varphi)^2 + \psi^\dagger[i\partial_0 - \epsilon(-i\partial)]\psi - g\partial\varphi\frac{i\psi^\dagger\overleftrightarrow{\partial}\psi}{2m}. \quad (5)$$

The low-energy parameters f_t , f and g are not constrained by the U(1) symmetries. Their values are not essential for the discussion of the phase diagram below. However, for the purpose of further applications, we point out that they are constrained by the Galilean invariance. Using the results of Refs. [15, 16], one can show that $f_t^2 = dn/d\mu$, $f^2 = n/m$, and $g = 1$.

Note that the interaction term $\psi^\dagger\psi[\dot{\varphi} + (\partial\varphi)^2/(2m)]$ is allowed, but is negligible when the number density of fermion quasiparticles is small, $\psi^\dagger\psi \ll n$. The fermion self-interaction $(\psi^\dagger\overleftrightarrow{\partial}\psi)^2$ is also irrelevant.

C. Phases near the splitting point

When $\alpha > 0$ the ground state may carry nonzero spatial gradient of φ or, in other words, nonzero superfluid velocity $\mathbf{v}_s = \partial\varphi/m$. This can be seen, e.g., from the fact that a state with an arbitrarily small density of fermions and $\mathbf{v}_s = 0$ has a negative superfluid density due to the divergent density of states at the Fermi surface [17]. Our task is to find, at each value of α (close to 0), the minimum of the free energy as a function of \mathbf{v}_s . Using Eqs. (4) and (5) we find the fermion dispersion relation in the presence of a uniform superfluid flow with velocity \mathbf{v}_s :

$$\epsilon_v(\mathbf{p}) = \epsilon_0 - \alpha p^2 + \beta p^4 + \mathbf{v}_s \cdot \mathbf{p} - H. \quad (6)$$

All levels with $\epsilon_v(\mathbf{p}) < 0$ are filled. The total free energy receives contributions from the superfluid flow and from the filled fermionic energy levels,

$$F(v_s) = \frac{\rho}{2}v_s^2 + \int \frac{d^3\mathbf{p}}{(2\pi)^3} \epsilon_v(\mathbf{p}) \theta(-\epsilon_v(\mathbf{p})). \quad (7)$$

Here $\rho = mn$, and $\theta(x)$ is the step function. Performing the integration, we find the free energy,

$$F(v_s) = \frac{1}{4(15\pi^2)^4} \frac{\alpha^5}{\rho^3\beta^7} f_h(x), \quad (8)$$

where we rescaled v_s and $(H - \Delta)$ by introducing dimensionless variables

$$x = \sqrt{2}(15\pi^2)^2 \frac{\rho^2\beta^{7/2}}{\alpha^{5/2}} v_s, \quad (9)$$

$$h = 2(15\pi^2)^2 \frac{\rho^2\beta^4}{\alpha^3} (H - \Delta). \quad (10)$$

The shape of $F(v_s)$ at a given H is captured by the function $f_h(x)$,

$$f_h(x) = x^2 - \frac{1}{x} \left[(h+x)^{5/2} \theta(h+x) - (h-x)^{5/2} \theta(h-x) \right], \quad (11)$$

at the corresponding h , which is shown in Fig. 3. For $h < h_1 \approx -0.067$ the absolute minimum of f is located at $x = 0$. When $h_1 < h < h_2 \approx 0.502$ the minimum switches to $x \neq 0$. When $h > h_2$, the minimum switches back to $x = 0$.

The change in the location of the minimum of f translates into two *first-order* phase transitions occurring at

$$\eta_{1,2} = 1 + \frac{h_{1,2}}{2(15\pi^2)^2} \frac{\alpha^3}{\rho^2\beta^4\Delta}. \quad (12)$$

The following picture emerges. At fixed $\kappa > \kappa_0$, as we increase η from 0 the ground state is an unpolarized superfluid (phase I) for $\eta < \eta_1$, until a phase transition at

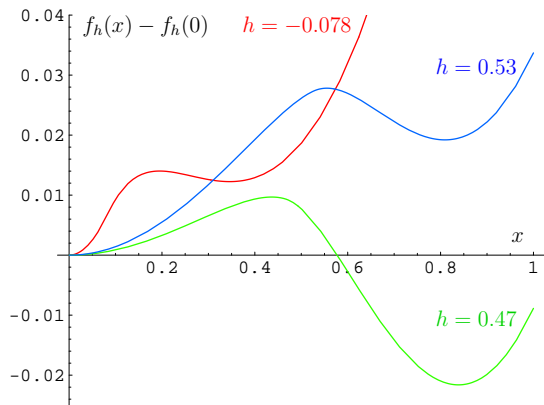


FIG. 3: Function $f_h(x)$ at three representative values of h .

$\eta = \eta_1$. Note that, since $h_1 < 0$, the phase transition occurs while H is still below the gap: $H_1 < \Delta$.

For $\eta_1 < \eta < \eta_2$ the ground state has nonzero superfluid velocity v_s (phase IV). It also contains fermionic quasiparticles filling an asymmetric region in the phase space [Figs. 4 and 5(a)]. The currents carried by the superfluid flow and by fermion quasiparticles cancel each other so that all currents (both total number and polarization) in the ground state are zero.

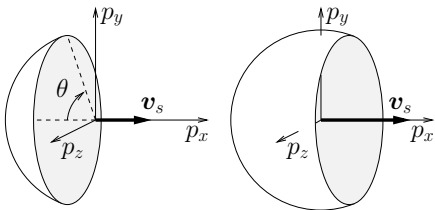


FIG. 4: Occupied fermion quasiparticle modes in phase IV near point S occupy a thin spherical cap with curvature radius $p = \sqrt{\alpha/(2\beta)}$. The angle θ increases from 80.4° at $\eta = \eta_1 + 0$ to 127.3° at $\eta = \eta_2 - 0$.

When $\eta > \eta_2$ the superfluid velocity switches back to zero. However, now $H > \Delta$, so there is a finite density of fermionic quasiparticles (phase III). At $\eta = \eta_2 + 0$ the fermions fill a thin spherical shell centered at $\mathbf{p} = 0$ [Fig. 5(b)]. As η increases, the shell thickens and at

$$\eta = \eta_3 \equiv \frac{\epsilon_0}{\Delta} = 1 + \frac{\alpha^2}{4\beta\Delta}, \quad (13)$$

or $H = \epsilon_0$, the shell turns into a solid ball [Fig. 5(c)]. This occurs at the dashed line on Fig. 1.

IV. GLOBAL TOPOLOGY OF THE PHASE DIAGRAM AND CONCLUDING REMARKS

In the region $\eta_1 < \eta < \eta_2$ where $v_s \neq 0$, the condensate function varies as e^{iqx} with $q \equiv 2mv_s \rightarrow 0$. This has the

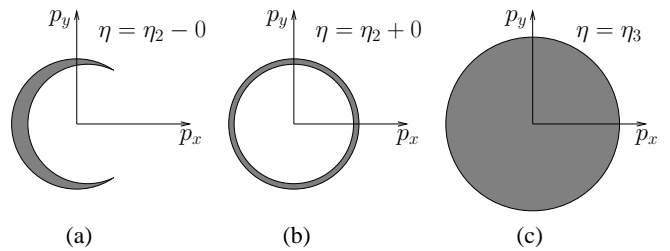


FIG. 5: Occupied quasifermion modes ($p_z = 0$ cross section) near point S in phase IV (a) and in phase III (b),(c).

same structure as the Fulde-Ferrell phase [12] in the BCS regime. Therefore, it is natural to expect that the region $\eta_1 < \eta < \eta_2$ near S is continuously connected to the FFLO region on the BCS side, as in Fig. 1.

In the BCS limit, the ground state is expected to be a crystal where $\Delta(\mathbf{x})$ is a superposition of several plane waves [18]. However, $\Delta(\mathbf{x})$ has to be a single plane wave near S . Indeed, v_s is small ($v_s \rightarrow 0$ as one approaches S), while the healing length is finite at S . If one tried to superimpose two plane waves to make a standing wave $\cos(qx)$, the absolute value of the condensate would vary on length scales much larger than the healing length, costing a large amount of energy. Therefore, one concludes that the FFLO region of the phase diagram is further subdivided into smaller regions with different patterns of breaking of rotational and translational symmetries.

The line separating the gapless superfluid phase III and the phase with nonzero v_s IV should end in a Lifshitz point L . It is known that in the vicinity of a Lifshitz point, the transition between the phase with spatially varying order parameter and that with constant order parameter *can* be second order when the broken symmetry is continuous [14]. If this is the case, then the first-order line $\eta = \eta_2(\kappa)$ should become second order at some value of κ before the point L . Another alternative is that the entire line from S to L is first order.

In the region between $\eta = \eta_2(\kappa)$ and $\eta = \eta_3(\kappa)$, but below the transition to the normal state (part of region III below the dashed curve on Fig. 1), the spectrum of low-energy excitations consists of the superfluid boson and the fermionic quasiparticles with momenta around *two* Fermi surfaces [the inner and the outer surfaces of the spherical shell in Fig. 5(b)]. This is the Sarma phase [19], which is unstable in the BCS limit but, as we found, is stable near the splitting point. This is interesting since previous examples of stabilized Sarma, or breached pairing, phase require quite special conditions [20].

Figure 1 describes the system at zero temperature T . At small $T \neq 0$ the phase diagram undergoes obvious modifications. Since the phases I and III have the same symmetry, the transition between them becomes an analytic crossover at $T \neq 0$. Similarly, the dashed line on Fig. 1 should turn into a crossover at $T \neq 0$. On the contrary, the phases II and III must remain separated by

a phase transition because the $U(1)$ symmetry is spontaneously broken in III and restored in II. Likewise, since the rotational symmetry undergoes spontaneous breakdown in phase IV, this phase must remain separated from all other phases by a phase transition.

The results obtained in this paper should be interesting for other physical systems with asymmetric fermion pairing, for example for the cores of neutron stars [21] or QCD at finite baryon and isospin chemical potentials [22]. We defer this investigation to future work.

Acknowledgments

The authors thank A. Bulgac, A. Kryjevski, H.-W. Hammer, and B. Spivak for discussions. This work was supported by DOE grants No. DE-FG02-00ER41132 and No. DE-FG0201ER41195 and the Alfred P. Sloan Foundation.

APPENDIX: GLOBAL STABILITY OF THE SPLITTING POINT

Near the splitting point we determined the minima of the free energy with respect to small perturbations around the superfluid state. By its nature, the effective field theory we applied cannot assert that the minima we study are global, i.e., stable with respect to large deviations from the state we considered. We must therefore employ different methods to assess the global stability of the point S . It is an important question since, as we show below, a mean-field approximation will likely show the normal, not superfluid, phase to be the globally stable state at the point S . Since the mean-field approximation is not a controllable approximation in the relevant regime $|\kappa| \lesssim 1$, other approaches are necessary to determine the global structure of the phase diagram.

Since the point S lies on the line $\eta = H/\Delta = 1$, the relevant comparison is between the pressure of the superfluid state $P_{\text{SF}}(\mu, H)$ at $H = \Delta$ and the pressure of the normal state $P_{\text{N}}(\mu, H)$ at the same H . We know that the normal state wins in the BCS limit, and the superfluid state wins in the BEC limit. Thus, there is a crossover at some value of κ_c

$$P_{\text{SF}}(\mu, \Delta) = P_{\text{N}}(\mu, \Delta) \quad \text{at } \kappa = \kappa_c. \quad (\text{A.1})$$

Assuming there is only one such crossover point, the stability of the point S requires that $\kappa_0 < \kappa_c$, i.e., that the splitting point S occurs while the superfluid state is still globally stable, as in Fig. 1.

Although no direct determination of κ_c has been made to date, Carlson and Reddy [11] have performed the pressure comparison at the unitarity point $\kappa = 0$, using a quantum Monte Carlo method. We shall now show that these results imply $\kappa_c \approx 0$, as well as that $\kappa_0 < 0$, and thus that the splitting point is globally stable.

At the point $\kappa = 0$ the only dimensionful parameters are the chemical potentials μ and H . The pressure of the superfluid phase is the same for all $H \in (0, \Delta)$ due to the gap, and, by dimensionality, is proportional to the pressure of a free two-component unpolarized Fermi gas at the same chemical potential,

$$P_{\text{SF}}(\mu, \Delta) = P_{\text{SF}}(\mu, 0) = \frac{P_{\text{free}}(\mu)}{\xi^{3/2}} \quad (\text{A.2})$$

where ξ is a universal dimensionless constant, conventionally defined as the ratio of the energy of the gas at unitarity and the energy of the noninteracting gas at the same density. $P_{\text{free}}(\mu) = 2(2m)^{3/2}/(15\pi^2)\mu^{5/2}$.

To find the pressure of the normal phase, we first notice that $\mu_{\downarrow} = \mu - \Delta < 0$ since $\Delta > \mu$ at unitarity (both in mean-field and in quantum Monte Carlo methods). Therefore the normal phase is a completely polarized (single-component—hence a factor 1/2 below) Fermi gas with $\mu_{\uparrow} = \mu + \Delta$, whose pressure is

$$P_{\text{N}}(\mu, \Delta) = \frac{1}{2}P_{\text{free}}(\mu_{\uparrow}) = \frac{1}{2} \left(1 + \frac{\Delta}{\mu}\right)^{5/2} P_{\text{free}}(\mu) \quad (\text{A.3})$$

The ratio of the pressures of the superfluid and the normal phases is therefore expressed in terms of two dimensionless quantities, ξ and Δ/μ ,

$$\frac{P_{\text{SF}}(\mu, \Delta)}{P_{\text{N}}(\mu, \Delta)} = \frac{2}{\xi^{3/2}} \left(1 + \frac{\Delta}{\mu}\right)^{-5/2} \quad \text{at } \kappa = 0. \quad (\text{A.4})$$

The Monte Carlo simulation of Ref. [11], finds $\xi \approx 0.42$ and $\Delta/\mu \approx 1.2$. Substituting into Eq. (A.4) one finds the ratio to be consistent with 1 within errors [11]. Comparing to Eq. (A.1) we conclude that $\kappa_c \approx 0$.

Carlson and Reddy [11] also found that at $\kappa = 0$ the fermion dispersion curve has a minimum at nonzero momentum, which means that the point $\kappa = 0$ is on the BCS side of the splitting point, i.e., $\kappa_0 < 0$. Since $\kappa_0 < 0 \approx \kappa_c$, we can conclude that the superfluid phase is still globally stable at the splitting point.

On the other hand, if we substituted into Eq. (A.4) the mean-field values $\xi \approx 0.59$, $\Delta/\mu \approx 1.16$ [23], we would find the ratio to be 0.64, i.e., the superfluid phase would appear to lose by a large margin at $\kappa = 0$. Therefore it is likely that in a mean-field calculation of the phase diagram the splitting point will be overshadowed by the normal phase. Instead of Fig. 1, in the regime $|\kappa| \lesssim 1$ one would then observe a single first-order transition (phase co-existence) line separating phases I and II. Qualitatively, it should be expected that a variational calculation overestimates the energy of the superfluid phase (i.e., the value of ξ). It is an interesting problem to see if the mean-field theory [9, 10] can be improved in the regime $|\kappa| \lesssim 1$ to describe the phase diagram correctly.

A calculation of the phase diagram using a two-channel Hamiltonian was reported recently [24]. It relies on a mean-field approximation which becomes controllable in the weak channel coupling (narrow resonance) limit. It

should be borne in mind that in this limit the effective range of the interaction diverges: $r_0 \gg n^{-1/3}$. This

limit [25] is therefore opposite to the zero-range limit we consider in this paper.

-
- [1] D. M. Eagles, Phys. Rev. **186**, 456 (1969).
 [2] A. J. Leggett, in *Modern Trends in the Theory of Condensed Matter* (Springer, Berlin, 1980).
 [3] P. Nozières and S. Schmitt-Rink, J. Low Temp. Phys. **59**, 195 (1985).
 [4] C. A. Regal, M. Greiner, and D. S. Jin, Phys. Rev. Lett. **92**, 040403 (2004).
 [5] M. Bartenstein, A. Altmeyer, S. Riedl, S. Jochim, C. Chin, J. Hecker Denschlag, and R. Grimm, Phys. Rev. Lett. **92**, 120401 (2004);
 [6] M. W. Zwierlein, C. A. Stan, C. H. Schunck, S. M. F. Raupach, A. J. Kerman, and W. Ketterle, Phys. Rev. Lett. **92**, 120403 (2004);
 [7] J. Kinast, S. L. Hemmer, M. E. Gehm, A. Turlapov, and J. E. Thomas, Phys. Rev. Lett. **92**, 150402 (2004);
 [8] T. Bourdel, L. Khaykovich, J. Cubizolles, J. Zhang, F. Chevy, M. Teichmann, L. Tarruell, S. J. J. M. F. Kokkelmans, and C. Salomon, Phys. Rev. Lett. **93**, 050401 (2004).
 [9] P. F. Bedaque, H. Caldas, and G. Rupak, Phys. Rev. Lett. **91**, 247002 (2003).
 [10] C.-H. Pao, S.-T. Wu, and S.-K. Yip, Phys. Rev. B **73**, 132506 (2006).
 [11] J. Carlson and S. Reddy, Phys. Rev. Lett. **95**, 060401 (2005).
 [12] P. Fulde and R. A. Ferrell, Phys. Rev. **135**, A550 (1964).
 [13] A. I. Larkin and Yu. N. Ovchinnikov, Zh. Exp. Teor. Fiz. **47**, 1136 (1964) [Sov. Phys. JETP **20**, 762 (1965)].
 [14] See, e.g., P. M. Chaikin and T. C. Lubensky, *Principles of Condensed Matter Physics* (Cambridge University Press, Cambridge, U.K., 1995).
 [15] M. Greiter, F. Wilczek, and E. Witten, Mod. Phys. Lett. B **3**, 903 (1989).
 [16] D. T. Son, e-print hep-ph/0204199.
 [17] A. G. Aronov and B. Z. Spivak, Fiz. Tverd. Tela (Leningrad) **17**, 2806 (1975) [Sov. Phys. Solid State **17**, 1874 (1975)].
 [18] J. A. Bowers and K. Rajagopal, Phys. Rev. D **66**, 065002 (2002).
 [19] G. Sarma, J. Phys. Chem. Solids **24**, 1029 (1963).
 [20] M. M. Forbes, E. Gubankova, W. V. Liu, and F. Wilczek, Phys. Rev. Lett. **94**, 017001 (2005).
 [21] M. Alford, C. Kouvaris, and K. Rajagopal, Phys. Rev. Lett. **92**, 222001 (2004).
 [22] D. T. Son and M. A. Stephanov, Phys. Rev. Lett. **86**, 592 (2001).
 [23] T. Papenbrock and G. F. Bertsch, Phys. Rev. C **59**, 2052 (1999).
 [24] D. E. Sheehy and L. Radzihovsky, Phys. Rev. Lett. **96**, 060401 (2006).
 [25] A. Schwenk and C. J. Pethick, Phys. Rev. Lett. **95**, 160401 (2005).